American Journal of Pathology, Vol. 153, No. 6, December 1998

Alterations of the p16-pRb Pathway and the Chromosome Locus 9p21–22 in Non-Small-Cell Lung Carcinomas

Relationship with p53 and MDM2 Protein Expression

Vassilis G. Gorgoulis,* Panayotis Zacharatos,* Athanassios Kotsinas,* Triantofillos Liloglou,† Aspasia Kyroudi,* Marinos Veslemes,‡ Antonios Rassidakis,‡ Thanos D. Halazonetis,§ John K. Field,† and Christos Kittas*

From the Departments of Histology and Embryology and Pulmonary Medicine,‡ School of Medicine, University of Athens, Athens, Greece; Roy Castle,† International Center for Lung Cancer Research, Liverpool, United Kingdom; and Department of Molecular Genetics,§ Wistar Institute, Philadelphia, Pennsylvania*

The p16-pRb and p53-MDM2 pathways represent vital cell cycle checkpoints. Recent studies provide evidence that these pathways are directly linked via MDM2-pRb interaction and p53 suppression of the *RB1* gene. In the present study we investigated the alterations of this G1 phase protein network using immunohistochemical and molecular methods in a series of 68 non-small-cell lung carcinomas (NSCLCs) and correlated the findings with clinicopathological features and prognosis of the patients. Aberrant expression (Ab) of p16 and pRb was observed in 33 (49%) and 27 (40%) of the carcinomas, respectively. Analysis of the region that encodes for p16 by deletion mapping, a polymerase chain reaction (PCR)-based methylation assay and PCR single-strand conformation polymorphism (SSCP) analysis revealed that deletions and transcriptional silencing by methylation might represent the main mechanisms of *CDKN2/p16*^{ink4a} inactivation in NSCLCs. The results of deletion mapping also suggest that other tumor suppressor genes may reside at the 9p21–22 region, which encodes for *CDKN2/MTS1/p16*^{ink4a}, *p14*^{ARF}, and *MTS2/p15*^{ink4b}. In addition, microsatellite instability was observed with a frequency of 16% in the 9p21–22 chromosome area. Overexpression (P) of p53 and MDM2 proteins was found in 39 (58%) and 47 (70%) of the cases, respectively. A highly significant association was observed between p53 overexpression and *p53* mutations ($P = 0.006$). Statistical analysis of the expression patterns of the biologically relevant molecules (p16/pRb, p53/MDM2, MDM2/pRb, and p53/pRb) showed coincident overexpression of p53 and MDM2 ($P = 0.04$) and that abnormal pRb was correlated with elevated levels of MDM2 ($P = 0.013$) and p53 ($P = 0.01$), respectively. We suggest that deregulated expression of these molecules may act synergistically. An important finding of the study was that multiple impairments (three and four molecules affected) of the p16/pRb/p53/MDM2 network occurred in a large proportion (43%) of the carcinomas. This finding in addition to the absence of correlation with clinical stage of the tumors suggests that multiple hits of this network may be a relatively early event in the development of a subset of NSCLCs. The relationship between the factors examined in the present study, clinicopathological features, and survival of the patients did not reveal any significant correlations with the exception of smoking, which was associated with microsatellite alterations (loss of heterozygosity and microsatellite instability) at the 9p21–22 locus ($P = 0.04$) and the immunophenotypes p53(P)/MDM2(P) ($P = 0.04$) and p16(Ab)/pRb(Ab)/p53(P)/MDM2(P) ($P = 0.03$), respectively. We suggest that in a subset of NSCLCs, simultaneous deregulation of the members of this network may represent one way of initiating the oncogenic procedure whereas in other NSCLC subgroups alternative pathways may play this role. ***(Am J Pathol 1998, 153:1749–1765)***

Non-small-cell lung cancer (NSCLC) represents one of the most frequent fatal human malignancies. Although tobacco and its derivatives are considered to be leading causes in NSCLC development, their underlying genetic targets are not yet completely clarified.[1] It is not surprising that alterations in the molecular machinery that controls transition from G1 to S phase might represent central events leading to NSCLC generation. In this respect, there is a strong body of evidence that cell-cycle regulators are involved in human cancer development.[2]

Accepted for publication August 31, 1998.

Address reprint requests to Dr. Gorgoulis Vassilis, Antaiou 53, Lamprini, Ano Patisia, Athens Greece, GR 11146.

Two of the most conspicuous molecules that emerge from ongoing studies in this field are the products of the *CDKN2/MTS1* gene, which is located on locus 9p21–22. The *CDKN2* gene encodes for two proteins: p16 and $p14^{ARF}$ (the human homologue of $p19^{ARF}$).[3] P16 consists of 156 amino acids (aa) and functions as an inhibitor of cyclin-dependent kinase 4 and 6 (CDK4 and CDK6).[2,4,5] CDK4- and CDK6-mediated phosphorylation of the retinoblastoma protein (pRb) is a critical step in cell cycle progression. The pRb protein ($p105^{RB1}$) is a 928-aa, 105-kd nuclear phosphoprotein encoded by the *RB1* tumor suppressor gene, which has been mapped to chromosomal region 13q14.2 (reviewed in Ref. 6). pRb phosphorylation is stimulated by cyclin D1 and inhibited by p16. Therefore, p16 and pRb are suggested to function in a single regulatory pathway of the cell cycle.[2] Unregulated phoshorylation of pRb by CDK4/6 due to either cyclin D1 overexpression or loss of functional p16 could lead to uncontrolled cellular proliferation.[2] The *CDKN2/p16*^{ink4a} gene product has been found to be nonfunctional in a high percentage of cell lines (75%) and various malignancies, suggesting that it is a candidate tumor suppressor protein.[2,7,8] The most common mechanisms for *CDKN2/p16*^{ink4a} inactivation appear to be homozygous deletions, mutations, loss of one allele, and inactivation of the other, probably due to hypermethylation.[2,7,8] Several reports have pointed out a difference in the frequency of *CDKN2/p16*^{ink4a} genetic alterations between cell lines and primary tumors.[8–11] Contamination of the cancerous tissue by the material derived from the surrounding stromal cells and artifactual or cellular adaptation during culture account for this difference. A similar situation has been described for *RB1* gene alterations in tumors.[12] Mutational inactivation of the *RB1* gene has been detected in a wide spectrum of malignancies, including retinoblastomas, small-cell lung, bladder, pancreatic, and breast carcinomas (reviewed in Ref. 6). The problem of evaluating p16 and pRb alterations, avoiding false positive results of the conventional molecular biology methods (polymerase chain reaction (PCR) and Southern blot) due to stromal contamination, can be circumvented by immunohistochemical methods that allow the investigation of protein abnormal expression at the single-cell level.

The data concerning the frequency and mechanisms of *CDKN2/p16*^{ink4a} gene inactivation in NSCLCs are controversial.[13–26] In reviewing the world literature published so far, we found six reports dealing with aberrant p16 immunoexpression and *in situ* distribution with percentages ranging from 27% to 67%.[13,20–22,24,25] Although most studies agree with the point that mutations are a rather rare mechanism of *CDKN2/p16*^{ink4a} inactivation (1% to 10%),[14–19,23,25] there is a great discrepancy regarding *CDKN2/p16*^{ink4a} gene deletion, with percentages ranging from 0% to 83%.[13,15–17,21–23,25] In addition, to the best of our knowledge, there are only two reports dealing with the methylation status of the *CDKN2/p16*^{ink4a} gene in NSCLCs.[25,26] On the other hand, inactivation of *RB1* gene has been shown in 9 to 38% of NSCLCs.[12,20–22,25–30] Recent, *in vitro* evidence has shown that *RB1* expression is negatively regulated by p53[31] and that MDM2 protein binds to the carboxy terminus of pRb, relieving pRb suppression of E2F transactivating function, thus permitting the cell to enter the S phase.[32] The *MDM2* gene is located on chromosome 12q13–14 and can generate various MDM2 protein isoforms. The full-length *MDM2* gene product p90 forms an autoregulatory feedback loop with p53 protein that seems to be vital for normal cell proliferation. Overexpression of MDM2 protein(s) has been observed in several human malignancies and associated with unfavorable prognosis (reviewed in Refs. 33 and 34). Recently, we reported that MDM2 protein isoforms are overexpressed and coexist with the mutant p53 protein (mt p53) in a subset of lung carcinomas, suggesting that this association may reflect a gain of function phenotype.[35–37]

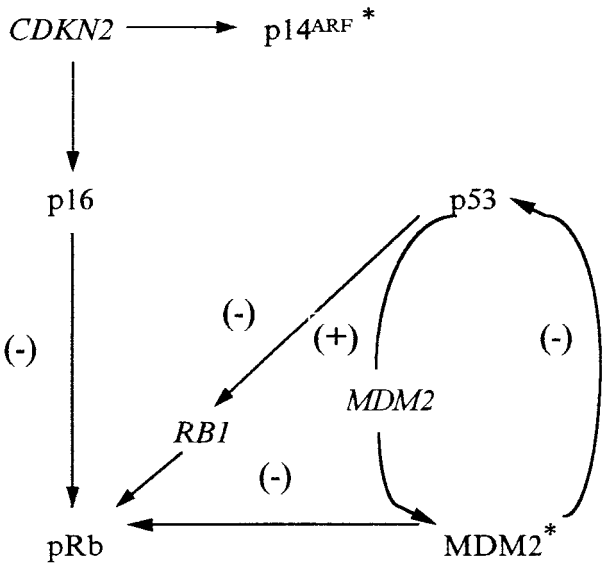

Figure 1. Schematic representation of the p16/pRb/p53/MDM2 protein network. p16 inhibits cyclin-dependent phosphorylation of pRb.[2] p53 and MDM2 form a feedback loop.[33] MDM2 binds the carboxy terminus of pRb, relieving pRb suppression of E2F transactivation function, thus permitting the cell to enter the S phase.[32] *RB1* is negatively regulated by p53.[31] *Recent evidence indicates that the other product of the *CDKN2* gene, $p14^{ARF}$ (the human homologue of $p19^{ARF}$), binds the carboxy terminus of MDM2, regulating its actions.[48,49]

The *in vitro* evidence mentioned above suggests that the p53-MDM2 duet is linked directly to the p16-pRb pathway (Figure 1). Alterations in this network may disrupt normal cell-cycle control. To investigate the involvement of this G1 protein network in non-small-cell lung carcinogenesis we examined, by immunohistochemical and molecular methods, its status in a series of 68 NSCLCs and correlated the findings with clinicopathological features and prognosis of the patients. Furthermore, we examined the state of the chromosomal region 9p21–22 by performing a mapping using a tight cluster of highly polymorphic microsatellite markers because there are indications that, in addition to *CDKN2/p16*^{ink4a} and *MTS2/p15*^{ink4b} tumor suppressor genes (TSGs), this region harbors other TSG(s)[38] (Figure 2a).

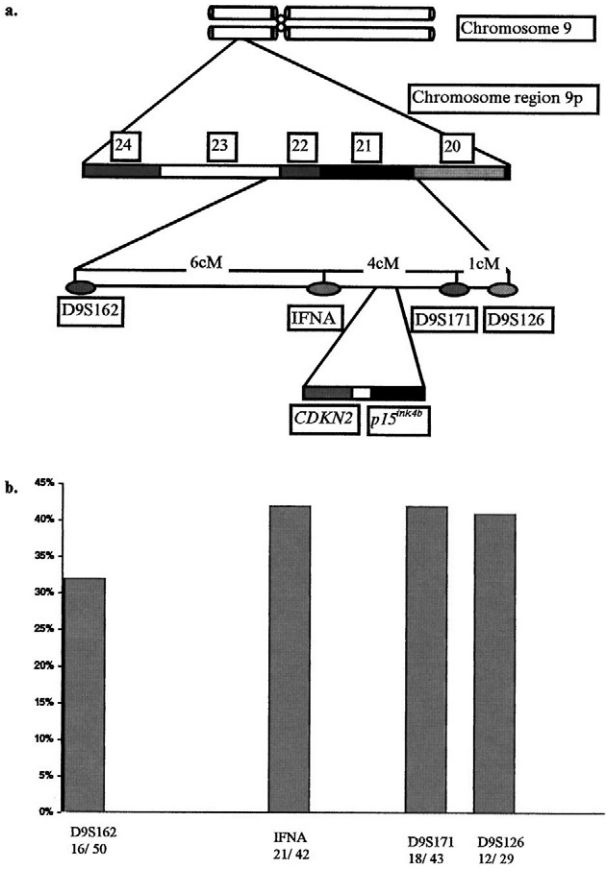

Figure 2. a: Schematic representation of the 9p21–22 region, the polymorphic microsatellite markers used in the study, and the location of the *CDKN2* and $p15^{ink4b}$ genes. b: Deletion frequencies observed at the *D9S162*, *IFNA*, *D9S171*, and *D9S126* loci.

Materials and Methods

Tissue Samples

Specimens from 68 NSCLCs were obtained in less than 15 minutes after surgery. Two samples of each tumor were taken. One was snap-frozen in liquid nitrogen and stored at −70°C; the other was formalin fixed and paraffin embedded (FFPE). In addition, adjacent normal tissue was included from each specimen examined. The patients had not undergone any chemo- or radiotherapy before surgical resection, thus avoiding up- and down-regulation of p53 and MDM2 proteins, respectively, due to DNA damage.[33] The material comprised 31 squamous cell carcinomas (SCLCs), 32 adenocarcinomas, and 5 undifferentiated large-cell carcinomas. Tumors were classified according to the World Health Organization criteria and TNM system.[39] Thirty carcinomas were stage I (10 T1/N0/M0, 2 T1/N1/M0, and 18 T2/N0/M0), 18 stage II (T2/N1/M0), and 20 stage III (6 T3–4, any N or M, and 14 N2, any T or M). The gender, age, and smoking habits of the patients are presented in Table 1.

Immunohistochemistry

Antibodies

For immunohistochemical analysis the following antibodies (Abs) were used: C-20 (IgG rabbit polyclonal; residues 137 to 156 of the carboxy terminus of p16) (Santa Cruz Biotechnology, Santa Cruz, CA), F-12 (IgG2a mouse monoclonal; residues 1 to 167 representing the full length p16) (Santa Cruz Biotechnology), Rb1 (IgG1 mouse monoclonal; residues 375 to 658 of pRb) (Dako, Glostrup, Denmark), DO7 (IgG2b mouse monoclonal; residues 1 to 45 of p53) (Dako), and 1B10 (IgM mouse monoclonal; carboxy terminus of MDM2) (Novocastra Laboratories, New Castle, UK).

Method

Five-micron paraffin sections of the lesions were mounted on poly-L-lysine-coated slides, dewaxed, rehydrated, and incubated for 30 minutes with 0.3% hydrogen peroxide to quench the endogenous peroxidase activity. Unmasking of p16, pRb, p53, and MDM2 proteins was carried out with the heat-mediated antigen retrieval (HMAR) method, as previously described,[35,36] when the monoclonal antibodies (MAbs) F-12, Rb1, DO7, and 1B10 were applied. The immunohistochemical assay for polyclonal (P)Ab C-20 did not include the antigen retrieval step. The sections were incubated with the antibodies at a 1:100 dilution at 4°C overnight. Biotin-conjugated secondary antibody was added at a 1:200 dilution for 1 hour at room temperature (RT). For color development we used 3,3′-diaminobenzidine tetrahydrochloride (DAB) and hematoxylin as counterstain.

Controls

The HeLa and Lo Vo cell lines with well defined p16 and pRb status, respectively, and lung carcinomas specimens from previous studies overexpressing p53 and MDM2 proteins were used as positive controls.[35,36] Mouse IgG1 MAb of unrelated specificity and the IgG fraction of normal rabbit serum were used as negative controls. Furthermore, the specificity of p16 staining with the PAb C-20 was tested by incubating the latter with the control peptide, C-20P, against which it was raised and applying it on the sections. Elimination of staining verified p16 positivity.

Evaluation: p16-pRb

For scoring the p16 and pRb staining patterns we used previously published criteria.[22,40] Cytoplasmic reactivity was disregarded, and only nuclear staining above any cytoplasmic background was considered as evidence of expression of the p16 and pRb proteins. The samples were divided into two categories: 1) p16 or pRb normal (No), when more than 90% of the tumor nuclei were stained and 2) p16 or pRb abnormal (Ab), when there was absence of nuclear staining in a portion of (heterogeneous) or in the entire (homogeneous) tumor section, whereas admixed non-neoplastic cells showed nuclear reactivity. A mosaic pattern of staining with absence of p16 or pRb reactivity in a proportion of tumor cells was not interpreted as abnormal.

Table 1. Summary of Clinicopathological Features, Immunohistochemical Results, and p53 and p16INK4a Gene Analysis

Clinicopathological features								Immunophenotypes by IHC			
Sample	Sex	Age (years)	Smoking	Histology	Stage	LN	Patients* follow-up	p16	pRb	p53	MDM2
19	M	70	YES	AD	I	NO	22+	No	No	N	N
20	M	66	YES	SQ	I	NO	22+	No	No	N	N
22	M	70	YES	AD	I	NO	22+	No	No	N	N
31	M	64	YES	AD	I	NO	10	No	No	N	N
51	M	48	YES	AD	II	YES	15	No	No	N	N
62	M	57	YES	SQ	I	NO	13	No	No	N	N
66	M	58	YES	SQ	II	YES	3	No	No	N	N
30	M	75	YES	UL	I	NO	20+	No	No	N	P
32	M	42	YES	AD	III	YES	18+	No	No	N	P
39	M	56	YES	SQ	III	YES	9	No	No	N	P
40	M	54	YES	UL	I	NO	18	No	No	N	P
43	M	60	NO	AD	II	YES	18+	No	No	N	P
44	M	72	NO	AD	III	YES	14	No	No	N	P
50	M	62	NO	AD	II	YES	17+	No	No	N	P
8	F	69	NO	AD	I	NO	22+	No	No	P	N
13	M	64	YES	SQ	III	YES	8	No	No	P	N
24	M	62	YES	SQ	I	NO	NA	No	No	P	N
52	M	72	YES	SQ	III	NO	17+	No	No	P	N
67	M	71	NO	AD	I	NO	10+	No	No	P	N
7	M	64	YES	SQ	II	YES	23+	No	No	P	P
10	F	68	YES	UL	II	YES	9	No	No	P	P
16	M	63	YES	AD	I	NO	7	No	No	P	P
18	M	73	YES	SQ	II	YES	11	No	No	P	P
59	M	65	YES	AD	I	NO	14+	No	No	P	P
25	M	63	NO	AD	I	NO	21+	No	Ab	N	N
33	M	59	YES	SQ	I	NO	14	No	Ab	N	P
49	M	53	NO	AD	I	NO	17+	No	Ab	N	P
53	M	60	YES	SQ	III	YES	15	No	Ab	P	N
1	M	57	YES	AD	III	YES	3	No	Ab	P	P
6	M	75	YES	SQ	II	YES	23+	No	Ab	P	P
28	M	60	YES	SQ	I	NO	21+	No	Ab	P	P
48	M	73	YES	SQ	III	NO	14	No	Ab	P	P
55	M	52	NO	AD	II	YES	10	No	Ab	P	P
57	M	58	YES	SQ	III	YES	8	No	Ab	P	P
36	M	57	NO	AD	III	YES	10	Ab	No	N	N
45	M	57	YES	AD	II	YES	18+	Ab	No	N	N
46	M	68	NO	AD	I	NO	17+	Ab	No	N	N
54	M	65	YES	SQ	I	NO	16+	Ab	No	N	N
3	M	61	YES	SQ	I	NO	25+	Ab	No	N	P
21	M	70	YES	SQ	III	YES	1	Ab	No	N	P
37	M	71	NO	AD	II	YES	12	Ab	No	N	P
41	M	67	YES	SQ	I	NO	18+	Ab	No	N	P
38	M	53	YES	SQ	III	YES	18+	Ab	No	P	N
5	M	61	YES	AD	III	YES	12	Ab	No	P	P
11	M	70	YES	SQ	I	NO	22+	Ab	No	P	P
17	M	64	YES	SQ	II	NO	22+	Ab	No	P	P
26	M	63	YES	AD	II	YES	17	Ab	No	P	P
42	M	76	YES	SQ	III	YES	18+	Ab	No	P	P
61	M	59	YES	AD	III	YES	14+	Ab	No	P	P
68	M	61	YES	SQ	II	YES	10+	Ab	No	P	P
23	M	79	YES	AD	II	YES	18	Ab	Ab	N	N
27	M	70	NO	AD	I	YES	14	Ab	Ab	N	P
34	M	63	YES	AD	I	NO	20+	Ab	Ab	N	P
4	M	60	YES	UL	I	NO	0	Ab	Ab	P	P
9	M	53	YES	AD	I	NO	23+	Ab	Ab	P	P
12	M	70	YES	SQ	I	NO	23+	Ab	Ab	P	P
14	M	74	YES	SQ	III	YES	8	Ab	Ab	P	P
15	M	69	YES	SQ	I	NO	22+	Ab	Ab	P	P
29	M	61	YES	UL	III	YES	0	Ab	Ab	P	P
35	M	67	YES	AD	I	YES	17	Ab	Ab	P	P
47	M	71	YES	SQ	I	NO	17+	Ab	Ab	P	P
56	M	58	YES	SQ	II	YES	11	Ab	Ab	P	P
58	M	52	NO	AD	II	YES	14+	Ab	Ab	P	P
60	M	64	YES	AD	III	YES	14+	Ab	Ab	P	P
63	F	60	YES	AD	III	NO	13+	Ab	Ab	P	P
64	M	62	YES	AD	I	NO	12+	Ab	Ab	P	P
65	M	56	YES	SQ	II	YES	12+	Ab	Ab	P	P
2	M	80	YES	SQ	III	YES	21	ND	ND	ND	ND

LN, lymph node metastases; IHC, immunohistochemical analysis; AD, adenocarcinoma; SQ, squamous cell carcinoma; UL, undifferentiated large-cell carcinoma; P, positive; N, negative; Ab, aberrant expression; No, normal expression; ND, not done; NA, not available; NM, normal methylation; HM, hypermethylation; +, possible mutation; −, no mutation.

*Numbers indicate months of survival after surgery; + indicates patient is alive.

Table 1. Continued

Molecular analysis					
p53 gene analysis				*p16^{INK4a}* gene analysis	
SSCP analysis	Defective exon	Gene mutation	Amino acid substitution	SSCP analysis	Methylation status
−				−	NM
+	9	ND		−	NM
−				−	NM
−				−	NM
−				−	NM
+	8	ND		−	NM
−				−	NM
−				−	NM
+	5	ND		−	NM
−				−	NM
−				−	NM
+	4	Codon 60, CCA → CCT	P → P	−	NM
+	6	ND		−	NM
−				−	NM
+	7	Codon 248, CGG → TGG	R → W	−	NM
+	7	Codon 248, CGG → CTG	R → L	−	NM
+	4	ND		−	NM
+	8	Codon 273, CGT → CAT	R → H	−	NM
−				−	NM
+	8	Codon 273, CGT → CTT	R → L	−	NM
+	4	Codon 93, CTG → ATG	L → M	−	NM
−				−	NM
+	7	Codon 230, ACC → AAC	T → N	−	NM
+	5	Codon 143, GTG → GCC	V → A	−	NM
−				−	NM
−				−	NM
−				−	NM
+	9	Codon 319, AAG → AAT	K → N	−	NM
−				−	NM
+	5	Codon 151, CCC → CAC	P → H	−	NM
+	5	ND		−	NM
+	7	Codon 237, ATG → ATA	M → I	−	NM
+	8	Codon 275, TGT → TTT	C → F	−	NM
+	5	Codon 153, CCC → CAC	P → H	−	NM
−				−	HM
−				−	NM
−				−	HM
−				−	HM
−				−	HM
−				−	HM
−				−	HM
+	4	Codon 110, CGT → CT	FS	−	HM
−				−	NM
+	7	Codon 244, GGC → TGC	G → C	−	NM
+	8	Codon 280, AGA → ATA	R → I	−	HM
−				−	NM
+	6	Codon 196, CGA → CCA	R → P	−	HM
+	5	Codon 157, GTC → TTC	V → F	−	HM
−				−	NM
−				−	HM
−				−	NM
+	8	ND		−	HM
−				−	HM
+	7	Codon 249, AGG → AGT	R → S	−	HM
+	7	Codon 238, TGT → TTT	C → F	−	NM
+	7	Codon 234, TAC → TGC	Y → C	−	NM
+	7	Codon 239, AAC → ACC	N → T	−	NM
+	5	Codon 163, TAC → TGC	Y → C	−	NM
+	4	Codon 69, GCT → GGT	A → G	−	NM
−				−	NM
−				−	HM
−				−	HM
−				−	HM
−				−	NM
−				−	NM
−				−	NM
−				−	NM
−				−	HM

Evaluation: p53-MDM2

Tumors were considered p53 or MDM2 positive (P) when more than 20% of tumor cells showed nuclear staining.[36] The other tumors were scored as p53 negative (N) or MDM2 negative (N).

Microdissection and DNA Extraction

DNA was extracted from adjacent 5-μm sections of frozen tumor specimens. Contiguous 5-μm sections were processed, and the first section was stained with hematoxylin and eosin to visualize the extent of the tumor cells within each sample. The boundaries of the cancerous tissue were delineated microscopically, and excess normal tissues were removed with sterile surgical blades, as previously described.[41] The remaining neoplastic material was digested in 500 μl of lysis solution: 50 mmol/L Tris/HCl (pH 8.0), 150 mmol/L NaCl, 5 mmol/L EDTA, containing 1% SDS and proteinase K (Boehringer Mannheim, Mannheim, Germany) at a final concentration of 100 μg/ml. Lysis was carried out at 55°C for 48 hours. Additional proteinase K (50 μg/ml) was added on each day of lysis. DNA was extracted using the phenol/chloroform/isoamyl alcohol method.[42]

Microsatellite Alteration (MA) Analysis of the Chromosomal Region 9p21–22

Method

DNA from normal and cancerous tissue was compared by PCR analysis of a tight cluster of highly polymorphic microsatellite markers spanning 11cM across 9p21–22 with the following order from telomeric to centromeric 9p (Figure 2a): *D9S162* (172 to 196 bp), *IFNA* (138 to 150 bp), *D9S171* (159 to 177 bp), and *D9S126* (226 to 250 bp). The 50-μl reaction mixture contained 100 ng of DNA, 10 mmol/L Tris/HCl, pH 8.8, 50 μmol/L KCl, 2.5 mmol/L $MgCl_2$, 0.1% Triton X-100, 200 μmol/L each dNTP (dATP, dCTP, dGTP, and dTTP), 1 μmol/L each primer pair (Research Genetics, Huntsville, AL) and 1.5 U of *Taq* DNA polymerase (Promega, Madison WI). The thermal cycle profile was denaturation at 95°C for 10 minutes before the addition of *Taq* polymerase followed by 30 cycles of 40 seconds at 95°C, 35 seconds at 56°C, and 30 seconds at 72°C. The products were analyzed on 10% polyacrylamide gels containing 10% glycerol and visualized by silver staining.[42]

Control

To determine whether the PCR product was a microsatellite region or not, electrophoresis on denaturing polyacrylamide gels was used. The bands that correspond to the microsatellite regions, due to the higher existence of dinucleotide repeats, are separated according to their molecular weight. Furthermore, all samples showing changes in microsatellite sequences were verified by subjecting the corresponding DNA sample to a second, independent PCR analysis. This as well as control PCR reactions lacking DNA were done to eliminate the chance of false positives due to PCR artifacts or sample contamination. Finally, for microsatellite instability (MI) determination we used previously published criteria.[43]

Methylation Analysis of the CDKN2/p16^{ink4a} *Gene*

Primers

A 239-bp fragment of exon 1a was amplified using the following primers, employing the Oligo Software v.4.01.: p16AU, 5′-GGAGAGGGGGAGAGCAGGCA-3′, and p16AD, 5′-CTCCAGAGTCGCCCGCCATC-3′.

Method

The inability of some restriction enzymes to cut methylated sequences was used to examine the methylation status of exon 1a. There are two *Hpa*II sites and one *Ksp*I site (both restriction enzymes are methylation sensitive) within exon 1a. One microgram of genomic DNA from matched normal and tumor samples was digested overnight with *Hpa*II and *Ksp*I as previously described.[44] Five microliters of the digested DNA solutions was used as template in a 50-μl reaction mixture containing 10 μmol/L Tris/HCl, pH 8.8, 50 μmol/L KCl, 1.5 mmol/L $MgCl_2$, 0.1% Triton X-100, 5% dimethylsulfoxide, 5% glycerol, 200 μmol/L each dNTP (dATP, dCTP, dGTP, and dTTP), 1 μmol/L each primer, and 1.5 U of *Taq* DNA polymerase (Promega). The thermal cycle profile was denaturation at 95°C for 10 minutes before the addition of *Taq* polymerase followed by 30 cycles of 1 minute at 95°C, 45 seconds at 57°C, and 45 seconds at 72°C. PCR products were electrophoresed in 2% agarose gels stained with ethidium bromide.

Evaluation–Controls

When exon 1a of the *CDKN2* gene is methylated, then the methylation-sensitive restriction enzyme fails to cut and a PCR product is obtained. For each specimen analyzed, undigested and non-methyl-sensitive *Msp*I-digested samples served as positive and negative controls, respectively, as previously described.[44] Finally, we evaluated as methylation-positive samples only the cases with reproducible results.

Single-Strand Conformation Polymorphism Analysis of CDKN2/p16^{ink4a} *Gene*

Primers

The primers used for methylation analysis of exon 1a and the following primers, designed by using the Oligo Software v.4.01., for exon 2 of *CDKN2/P16*^{ink4a} (419-bp PCR-amplified fragment) were used for mutation analy-

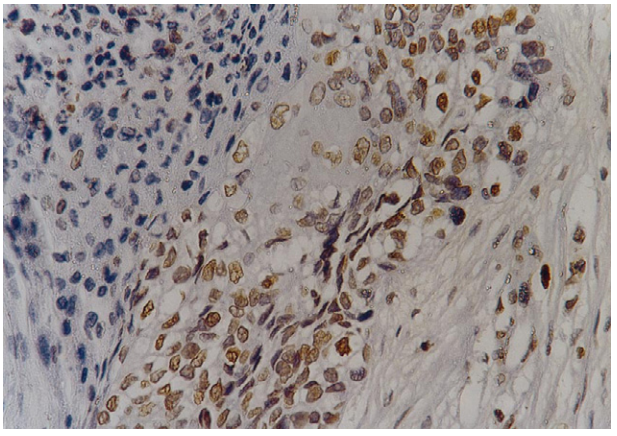

Figure 3. Squamous cell lung carcinoma with heterogeneous aberrant p16 expression (see Materials and Methods). Streptavidin-biotin peroxidase technique with F-12 anti-p16 antibody (see Materials and Methods) and hematoxylin counterstain; magnification, ×500.

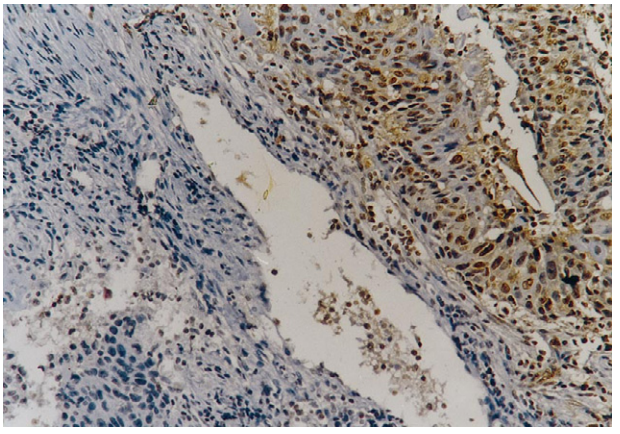

Figure 4. Squamous cell lung carcinoma with heterogeneous aberrant pRb expression (see Materials and Methods). Streptavidin-biotin peroxidase technique with Rb1 anti-pRb antibody (see Materials and Methods) and hematoxylin counterstain; magnification, ×125.

sis: p16BU, 5′-GGCTCTGACCATTCTGTTCTCTC-3′, and p16BD, 5′-GGCTGAACTTTCTGTGCTGG-3′.

Method

Single-strand conformation polymorphism (SSCP) was performed on normal and tumor-tissue-derived DNA as previously described.[45]

Nested-PCR/SSCP Analysis of the p53 *Gene*

The method was performed on matched normal and tumor DNA as previously described.[45] Briefly, a 2.9-kb *p53* gene fragment, which contains exons 4 to 9, was amplified,[36,37] as previous studies have shown that the majority of p53 mutations, in lung carcinomas, are found in this region. Individual exons 4–9 were further amplified by PCR, and nested products were analyzed with SSCP. Exons that showed mobility shifts were further analyzed with automated sequencing.

Automated Sequencing of the p53 *Gene*

PCR Amplification

Exons that harbored putative mutations were amplified with primers previously described[37] that were tailed with M13 forward and reverse primers. Reactions were performed on a PEC 480 thermal cycler block in 100-μl reactions (10 mmol/L Tris/HCl, pH 9.0, 50 mmol/L KCl, 2.5 mmol/L $MgCl_2$, 0.1% Triton X-100, 200 μmol/L dNTPs, 1 μmol/L each primer, 2.5 U of *Taq* (Promega), and 100 ng of genomic DNA) for 30 cycles of 1 minute at 94°C, 40 seconds at 56°C (for exons 4 and 7; 50°C for exons 5, 6, and 8; and 44°C for exon 9), and 40 seconds at 72°C.

Purification of PCR Product

The PCR products were purified with QIAquick Gel Extraction kit (QIAGEN, Hilden, Germany) according to the manufacturer's instructions and then quantitated by agarose gel electrophoresis after comparison with known amounts of standard DNA fragments.

Automated Sequencing

Cycle sequencing was performed on GeneAmp PCR System 9600 (Perkin-Elmer, Norwalk, CT) using fluorescently labeled M13 forward and reverse primers with Ampli*Taq* DNA polymerase, FS (*Taq*-FS, Perkin-Elmer/Applied Biosystems Division, Foster City, CA) according to the manufacturer's directions. Briefly, purified DNA (0.1 to 1 mg) was mixed with 2 μl of 10X FS buffer (125 mmol/L Tris/HCl, pH 9.5, 50 mmol/L $(NH_4)_2SO_4$, 150 mmol/L $MgCl_2$), 2 pmol of Cy-5-labeled primer, and 1 μl of FS enzyme in 20-μl reactions. Five-microliter aliquots of the above were mixed with 2 μl of each termination solution (a mixture of deoxy- and dideoxy-ribonucleotides provided by Perkin-Elmer). Sequencing reactions were run under the following conditions: 2 minutes of initial denaturation at 95°C followed by 25 cycles at 95°C for 30 seconds and 50°C for 30 seconds. At the end, 4 μl of

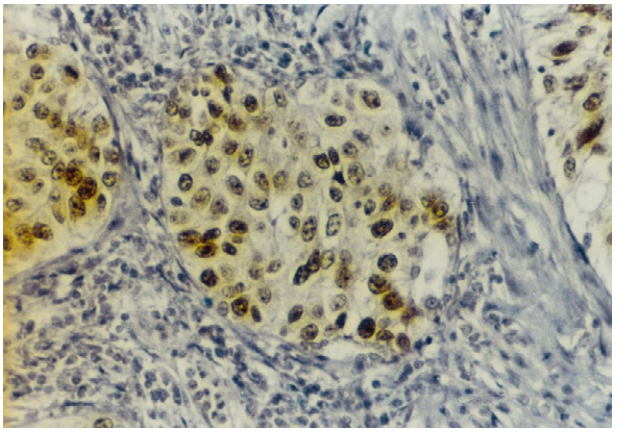

Figure 5. Squamous cell lung carcinoma with MDM2 protein overexpression. Streptavidin-biotin peroxidase technique with 1B10 anti-MDM2 antibody (see Materials and Methods) and hematoxylin counterstain; magnification, ×500.

Table 2. Relationship of the Immunohistochemical Results with Various Clincopathological Parameters

	Clinicopathological data												
	Smoking			Histology				LN			Stage			
IHC	Yes	No	*P*	SQ	AD	UL	*P*	Yes	No	*P*	I	II	III	*P*
p16														
No	26	8	0.57	14	17	3	0.8011	16	18	0.537	16	9	9	0.9
Ab	28	5		16	15	2		19	14		14	9	10	
Total	54	13		30	32	5		35	32		30	18	19	
pRb														
No	32	8	0.86	18	19	3	0.9986	21	19	0.843	17	12	11	0.77
Ab	22	5		12	13	2		14	13		13	6	8	
Total	54	13		30	32	5		35	32		30	18	19	
p53														
N	19	9	0.054	9	17	2	0.1817	13	15	0.57	16	7	5	0.2
P	35	4		21	15	3		22	17		14	11	14	
Total	54	13		30	32	5		35	32		30	18	19	
MDM2														
N	15	5	0.67	9	11	0	0.2951	8	12	0.297	11	4	5	0.5
P	39	8		21	21	5		27	20		19	14	14	
Total	54	13		30	32	5		35	32		30	18	19	

Ab, abnormal expression; No, normal expression; SQ, squamous cell carcinoma; AD, adenocarcinoma; UL, undifferentiated large-cell carcinoma; P, positive; N, negative.

formamide stop solution was added, and samples were heated at 95°C for 2 minutes and loaded on ALF Express sequencing gels (Pharmacia, Uppsala, Sweden). Gels were run on an automated DNA sequencer (ALF Express, Pharmacia).

Statistical Analysis

Statistical analysis was based on χ^2 with Yates' correction. An additional two-tailed Fisher's exact test was used only when the number of samples in any cell of a given statistical table was five or fewer. Multiple regression analysis was performed to examine the possible relationship between the biologically relevant and combined immunoprofiles and clinicopathological parameters. The computations were carried out using the Statistica software package. The survival curves were calculated by the Kaplan-Meier method using the SPSS software package. The statistical difference was considered significant if the *P* value was <0.05.

Results

Immunohistochemistry

Immunohistochemical Expression of p16, pRb, p53, and MDM2 Proteins and Relationship with Various Clinicopathological Parameters

Immunohistochemical (IHC) analysis revealed aberrant expression of p16 and pRb in 33 (49%) and 27 (40%) of the 67 carcinomas, respectively (Figures 3 and 4). There was concordance of p16 staining with both antibodies used. Reactivity for p53 and MDM2 was observed in 39 (58%) and 47 (70%) of the tumors, respectively (Figure 5). P16, pRb, p53, and MDM2 results and their relationship with smoking habits, histology, lymph node status, and stage are presented in Table 2. As shown in Table 2, the percentages of p16, pRb, and MDM2 expression are comparable between SCLCs and adenocarcinomas, whereas p53 staining in adenocarcinomas is lower (47%) as compared with SCLCs (70%). Statistical analysis did not reveal any significant correlations with the exception of a probable association between p53 overexpression and smoking (35/54 (65%) *versus* 4/13 (30%); $P = 0.054$).

Relationship of the Expression of the Biologically Relevant Molecules (p16/pRb, p53/MDM2, MDM2/pRb, and p53/pRb)

The relationship of the biologically relevant molecules examined in the present work is illustrated in Figure 1. Statistical analysis of the immunostaining patterns showed that 1) MDM2 overexpression was accompanied by p53 overexpression (MDM2(P)/p53(P) 32/39 (82%) *versus* MDM2 (P)/p53(N)15/28 (54%); $P = 0.02$) and 2) abnormal detection of pRb was significantly associated with increased production of MDM2 and p53 proteins, respectively (pRb(Ab)/MDM2(P) 24/47 (51%) *versus* pRb(Ab)/MDM2(N) 3/20 (15%); $P = 0.013$; and pRb(Ab)/p53(P) 21/39 (54%) *versus* pRb(Ab)/p53(N) 6/28 (21%); $P = 0.01$). Although p16-pRb expression patterns did not reveal any significant correlations, an inverse relationship between p16 and pRb was observed in 26 (39%) of the 67 carcinomas (p16(Ab)/pRb(No), 10/67 (15%), or p16(No)/pRb(Ab), 16/67 (24%)). Furthermore, coincident aberrant expression of p16 and pRb was observed in 17 cases (25%).

Relationship of the Biologically Relevant Immunoprofiles with Various Clinicopathological Parameters

The relationship of the biologically relevant immunophenotypes, p16/pRb, p53/MDM2, MDM2/pRb, and p53/pRb with smoking habits, histology, lymph node status,

Table 3. Relationship of the Biologically Relevant Immunoprofiles with Various Clinicopathological Parameters

	Clinicopathological data												
	Smoking			Histology				LN			Stage			
IHC	Yes	No	*P*	SQ	AD	UL	*P*	Yes	No	*P*	I	II	III	*P*
p16/pRb														
No/No	19	5	0.7	9	12	3	0.5321	11	13	0.77	12	7	5	0.8
No/Ab	7	3		6	4	0		5	5		4	2	4	
Ab/No	13	3		9	7	0		10	6		5	5	6	
Ab/Ab	15	2		6	9	2		9	8		9	4	4	
Total	54	13		30	32	5		35	32		30	18	19	
p53/MDM2														
N/N	10	3	0.04	4	8	0	0.4863	5	8	0.59	8	4	1	0.1
P/N	5	2		5	2	1		3	4		3	0	4	
N/P	9	6		5	9	1		8	7		8	3	4	
P/P	30	2		16	13	3		19	13		11	11	10	
Total	54	13		30	32	5		35	32		30	18	19	
pRb/MDM2														
No/N	12	4	0.9	7	9	0	0.8247	5	11	0.15	10	3	3	0.4
No/P	19	4		10	10	3		15	8		7	9	7	
Ab/N	3	1		2	2	0		3	1		1	1	2	
Ab/P	20	4		11	11	2		12	12		12	5	7	
Total	54	13		30	32	5		35	32		30	18	19	
p53/pRb														
N/No	16	6	0.871	8	12	2	0.4952	11	11	0.757	11	6	5	0.395
P/No	16	2		10	7	1		10	8		6	6	6	
N/Ab	3	3		1	5	0		2	4		5	1	0	
P/Ab	19	2		11	8	2		12	9		8	5	8	
Total	54	13		30	32	5		35	32		30	18	19	

Ab, abnormal expression; No, normal expression; SQ, squamous cell carcinoma; AD, adenocarcinoma; UL, undifferentiated large-cell carcinoma; P, positive; N, negative.

and stage are summarized in Table 3. Statistical analysis showed a probably significant association between the p53(P)/MDM2(P) pattern and smoking (30/54 (56%) *versus* 2/13 (15%); $P = 0.04$, Table 3). Next we examined the association between p16/pRb/p53/MDM2 profile and clinicopathological characteristics of the carcinomas. The tumors were divided into four groups according to the number of alterations detected (Table 4).

As shown, alterations in three and four components of the network (Figure 1) were observed in 15 (22%) and 14 (21%) of the cases, respectively. A probably significant correlation was found between the p16(Ab)/pRb(Ab)/p53(P)/MDM2(P) immunoprofile and smoking (13/54 (24%) *versus* 1/13 (8%); $P = 0.03$, Table 4).

Microsatellite Alteration Analysis of the Chromosomal Region 9p21–22

For microsatellite alteration (MA) analysis we used a tight cluster of highly polymorphic microsatellite markers spanning 11cM across 9p21–22 with the following order from telomeric 9p to centromeric 9p (Figure 2a): *D9S162, IFNA, D9S171*, and *D9S126.*

Of 68 cases, 50 (74%) were informative for *D9S162*, 42 (62%) for *IFNA,* 43 (63%) for *D9S171*, and 29 (43%) for *D9S126*. Thirty-five (51%) NSCLCs displayed loss of heterozygosity (LOH) at one or more markers (Figures 6 and 7). The deletion frequencies for each marker are presented in Figure 2b. The results were further categorized

Table 4. Relationship of the Combined Immunoprofile with Various Clinicopathological Parameters

p16/pRb/p53/MDM2 pattern	Clinicopathological data													
	Smoking			Histology				LN			Stage			
	Yes	No	*P*	SQ	AD	UL	*P*	Yes	No	*P*	I	II	III	*P*
Alterations (0)	6	0		3	3	0		2	4		4	2	0	
Alterations (1+)	10	8		5	11	2		8	10		9	3	6	
Alterations (2+)	12	2	0.03	8	5	1	0.57	8	6	0.6	6	5	3	0.5
Alterations (3+)	13	2		8	7	0		10	5		4	5	6	
Alterations (4+)	13	1		6	6	2		7	7		7	3	5	
Total	54	13		30	32	5		35	32		30	18	19	

SQ, squamous cell carcinoma; AD, adenocarcinoma; UL, undifferentiated large-cell carcinoma.

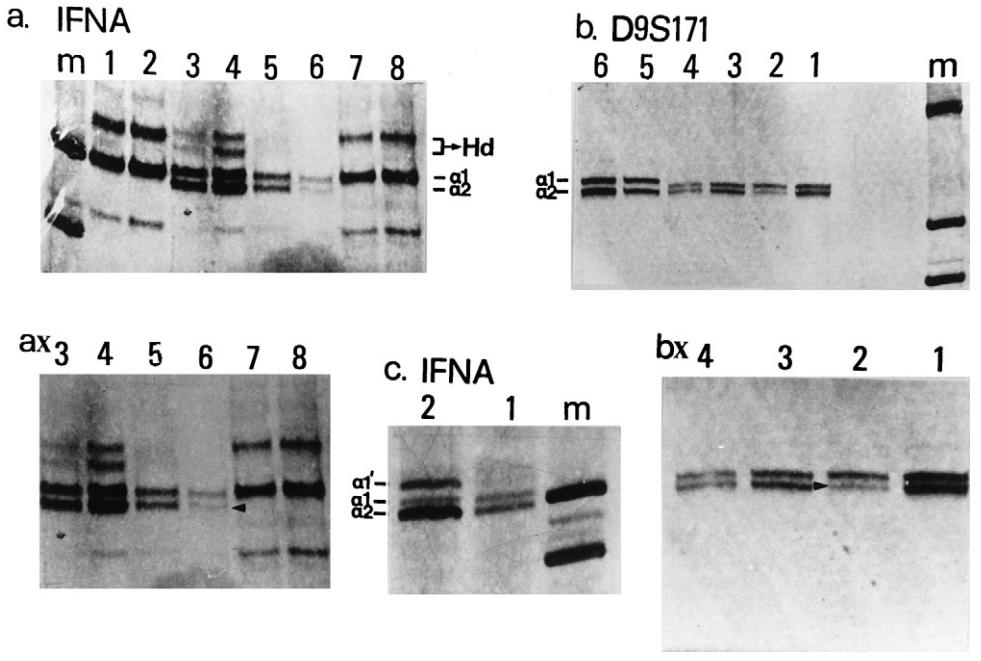

Figure 6. Representative results of deletion mapping and microsatellite instability analysis (MI) with chromosome markers *IFNA* and *D9S171*. a: Lane m , marker (PUC19/*Sau*3AI); lanes 1, 2, 7, and 8, matched normal-tumor samples (cases 28 and 31) with no polymorphism at the *IFNA* locus; lanes 3 and 4, matched normal-tumor samples (case 49) with polymorphism at the *IFNA* locus (a1 and a2 alleles; Hd, heteroduplex but no indication of loss of heterozygosity (LOH); lanes 5 and 6, matched normal-tumor samples (case 61) with polymorphism at the *IFNA* locus and LOH. ax: Magnification of lanes 5 and 6; LOH is shown with arrowhead. b: Lane m, marker (PUC19/*Sau*3AI); lanes 3 to 6, matched normal-tumor samples (cases 49 and 54) with polymorphism at the *D9S171* locus but no indication of LOH; lanes 1 and 2, matched normal-tumor samples (case 15) with polymorphism at the *D9S171* locus and LOH. bx: Magnification of lanes 1 and 2; LOH is shown with arrowhead. c: Lane m, marker (PUC19/*Sau*3AI); lanes 1 and 2, matched normal-tumor samples (case 3). The tumor sample showed at the *IFNA* locus MI, which is demonstrated as an aberrant band (a1′). The band at the position of the a1 allele is possibly due to DNA contamination from the non-neoplastic surrounding cells.

into three groups: group LOH(c), the cases that demonstrated a central LOH, at the *IFNA* and/or *D9S171* loci indicating a possible deletion of the *CDKN2* gene; group LOH(f), the patients with chromosomal abnormalities at the flanks upstream of *IFNA* and/or downstream of *D9S171*; and group LOH(−), the cases with no indication of LOH and/or noninformative (NI) samples. Of the 68 patients, 27 (40%) were placed in group LOH(c), 9 (13%) in group LOH(f), and 32 (47%) in group LOH(−) (Figure 8).

Apart from chromosomal deletions, 11 (16%) patients demonstrated MAs, which appeared as an expansion or a compression of a single band or a ladder of bands (Figure 6). These alterations were characterized as microsatellite instability (MI), as previously described.[43,47] MI was observed in all of the microsatellite loci examined, and it was more frequent in SCLCs (8/30, 27%) than in adenocarcinomas (3/32, 9%). In two of these cases, MI co-existed with LOH. Thus, in total, MAs (LOH plus MI) at the 9p21–22 chromosomal region were detected in 44 (65%) cases.

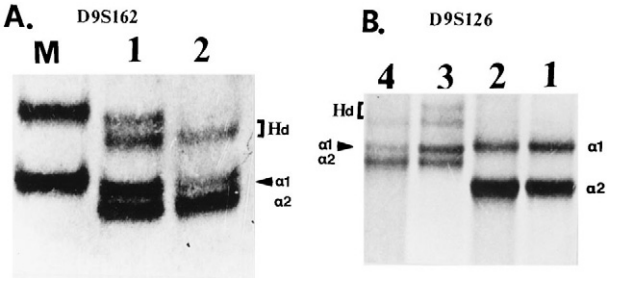

Figure 7. Representative results of deletion mapping with chromosome markers *D9S162* and *D9S126*. A: Lane M, marker ($\phi\chi$174/*Hae*III); lanes 1 and 2, matched normal-tumor samples (case 11) with polymorphism at the *D9S162* locus and LOH (arrowhead). a1 and a2, alleles; Hd, heteroduplex). B: Lanes 1 and 2, with polymorphism at the *D9S126* locus but no indication of LOH; lanes 3 and 4, matched normal-tumor samples (case 12) with polymorphism at the *D9S126* locus and LOH (arrowhead). a1 and a2, alleles; Hd, heteroduplex.

In relation to clinicopathological parameters we observed a probably significant association between smoking and MAs at the examined region (MAs/smoking(+), 36/55 (65%), *versus* MAs/smoking(−), 4/13 (31%); $P = 0.04$).

Interestingly, LOH and MAs were more frequent in the cases with abnormal pRb expression (LOH/pRb(Ab), 19/27 (70%), *versus* LOH/pRb(No), 16/40 (40%); $P = 0.02$, and MAs/pRb(Ab), 20/27 (74%), *versus* MAs/pRb(No), 19/40 (48%); $P = 0.05$). Finally, we examined the relationship between LOH(c) and MDM2 protein status because there is current evidence that demonstrates that $p14^{ARF}$ is involved in the stabilization of MDM2.[48,49] However, no significant association was observed (LOH(c)/MDM2(P), 21/48 (44%), *versus* LOH(c)/MDM2(N), 5/19 (26%); $P = 0.29$).

CDKN2/$p16^{ink4a}$ *Gene Methylation Analysis*

To address further the molecular basis of aberrant p16 expression we examined the methylation status of *CDKN2/*$p16^{ink4a}$ exon 1a, which has been shown to cor-

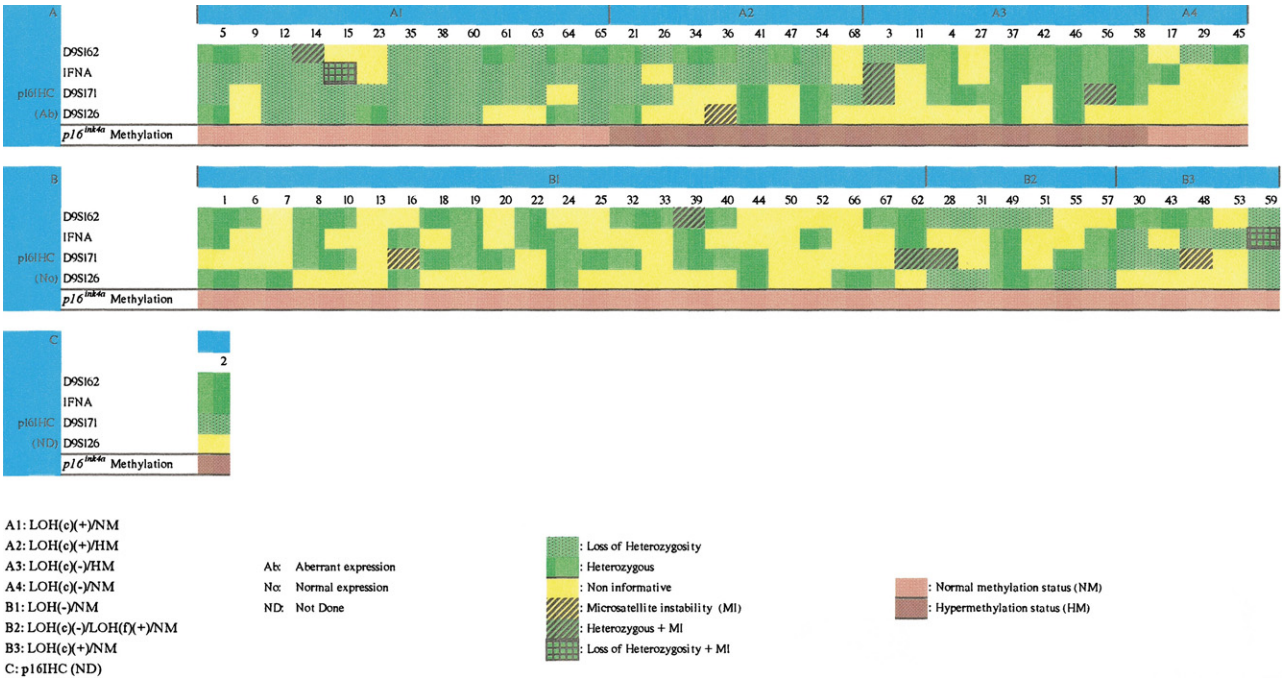

Figure 8. Relationship between p16 immunohistochemistry, microsatellite alterations at the 9p21–22 chromosome region and methylation of the *CDKN2/p16*^{ink4a} gene.

relate strongly with transcriptional silencing of the gene.[50] Briefly, after DNA digestion with methylation-sensitive and -insensitive restriction enzymes, PCR amplification was performed. When exon 1a is methylated, a PCR product is obtained. Using this procedure, we found that 18 (26%) of 68 carcinomas analyzed exhibited *de novo* methylation of exon 1a (Figure 9). Methylation patterns did not vary between *Hpa*II and *Ksp*I. Furthermore, all normal tissues were unmethylated within the examined regions.

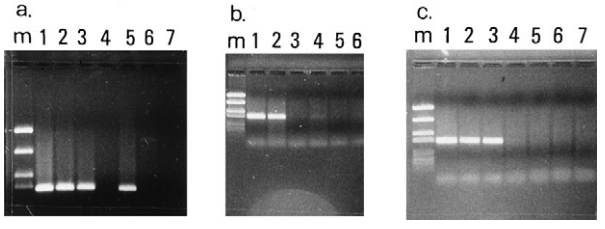

Figure 9. Representative results of the PCR-based methylation assay. **a**: *De novo* methylation of *CDKN2/p16*^{INK4a} exon 1a in a undifferentiated NSCLC (case 4). **Lane m**, marker (PUC19/*Sau*3AI); **lane 1**, undigested PCR product from HeLa cell line included as control; **lanes 2** and **3**, undigested PCR products from matched normal-tumor sample; **lanes 4** and **5**, digestion with methylation-sensitive enzyme *Hpa*II revealed that *CDKN2/p16*^{ink4a} in nontumor tissue is unmethylated as no amplification by PCR is seen, whereas in the tumor, *CDKN2/p16*^{ink4a} is methylated as digestion does not affect amplification; **lanes 6** and **7**, digestion with non-methylation-sensitive enzyme *Msp*I affects amplification in normal and tumor tissue. **b**: *De novo* methylation of *CDKN2/p16*^{ink4a} exon 1a in a squamous cell lung carcinoma (case 11). **Lane m**, marker (PUC19/*Sau*3AI); **lanes 1** and **2**, undigested PCR products from matched normal-tumor sample; **lanes 3** and **4**, digestion with methylation-sensitive enzyme *Ksp*I revealed that *CDKN2/p16*^{ink4a} in nontumor tissue is unmethylated as no amplification by PCR is seen, whereas in the tumor, *CDKN2/p16*^{ink4a} is methylated as digestion does not affect amplification; **lanes 5** and **6**, digestion with non-methylation-sensitive enzyme *Msp*I affects amplification in normal and tumor tissue. **c**: An adenocarcinoma with no indication of *CDKN2/p16*^{ink4a} methylation (case 25). **Lane m**, marker (PUC19/*Sau*3AI); **lane 1**, undigested PCR product from HeLa cell line; **lanes 2** and **3**, undigested PCR products from the sample; **lanes 4** and **5**, digestion with methylation-sensitive enzyme *Ksp*I; **lanes 6** and **7**, digestion with non-methylation-sensitive enzyme *Msp*I.

SSCP Analysis of the p53 *and* CDKN2/p16^{ink4a} *Genes*

To assess point mutations and short nucleotide sequence insertions or deletions of the *p53* gene, we analyzed with SSCP exons 4 to 9, obtained by nested PCR, from tumor-derived and normal-tissue-derived DNA. The same procedure was carried out with exons 1a and 2 of the *CDKN2/p16*^{ink4a} gene.

Tumor-specific mobility shifts were observed in 24 (61.5%) and 7 (25%) of the p53 immunohistochemically positive and negative cases, respectively. A highly significant association was observed between *p53* gene mutations and p53-positive staining (*p53* mt(+)/p53 IHC(+), 24/39 (61.5%), *versus p53* mt(+)/p53 IHC(−), 7/28 (25%); $P = 0.006$). The data from the SSCP and sequencing analysis (Figure 10) are presented in detail in Table 1.

No tumor-specific migrational shifts were observed in any of the NSCLCs by PCR-SSCP analysis of exons 1a and 2 of *CDKN2/p16*^{ink4a}.

Relationship between p16 Immunohistochemical Findings, Microsatellite Alterations at the 9p21–22 Locus, and Methylation Status of the CDKN2 *Gene (Figure 8)*

The cases with abnormal p16 (Ab) expression were placed in group A and the cases with normal p16 staining

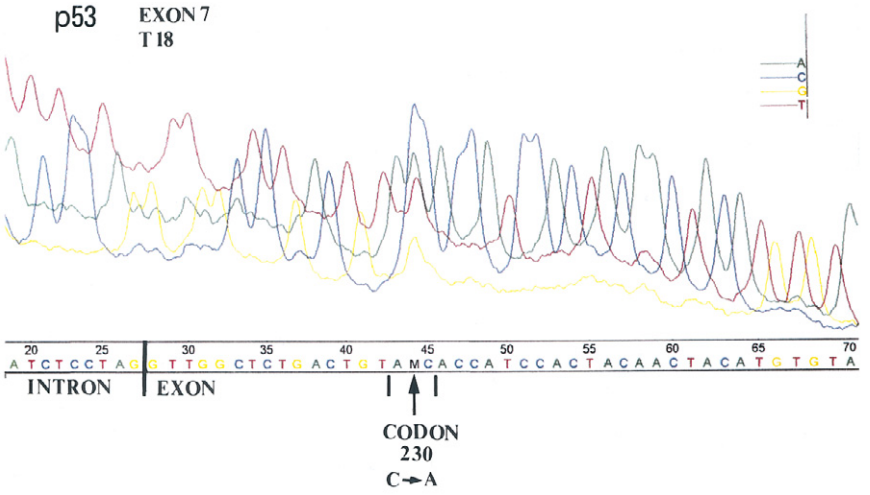

Figure 10. Representative automated sequencing in a squamous cell lung carcinoma (case 18) with SSCP mobility shift in exon 7. The position of the *p53* mutation is located at codon 230 and changes ACC (T) to AAC (N).

(No) in group B. Group A was further divided into four subgroups according to the LOH(c) and methylation analysis results and group B into three subgroups according to the LOH status.

Statistical analysis revealed a strong correlation between aberrant expression of p16 protein, LOH, and MAs at the 9p21–22 locus, respectively (LOH/p16(Ab), 24/33 (73%), *versus* LOH/p16(No), 11/34 (32%); $P = 0.002$, and MAs/p16(Ab), 25/33 (76%), *versus* MAs/p16(No), 14/34 (41%); $P = 0.008$. This association was even higher in the patients of group LOH(c) (LOH(c)/p16(Ab), 21/33 (64%), *versus* LOH(c)/p16(No), 5/34 (15%); $P = 0.0001$). All of the cases with *de novo CDKN2/p16*^{ink4a} methylation were accompanied with abnormal p16 staining (subgroups A2 and A3). In six methylated samples of subgroup A3 (cases 4, 27, 37, 42, 46, and 58) we did not notice microsatellite alterations in the 9p21–22 chromosomal region whereas in subgroup A2 *de novo* methylation of *CDKN2/p16*^{ink4a} was accompanied by LOH(c). Interestingly, the samples that comprised subgroup A4 did not show either LOH(c) or SSCP tumor-specific shifts or abnormal methylation status of *CDKN2/p16*^{ink4a}.

Survival Analysis

The survival analysis (follow-up duration up to 25 months) using the Kaplan-Meier method did not demonstrate any statistically significant association between patient outcome, individual abnormalities of the network proteins (including p53 mutations), various immunoprofiles, and alterations at the 9p21–22 chromosome region, respectively.

Discussion

To the best of our knowledge, the information of our study, which deals with alterations of the p16/pRb/p53/MDM2 protein network (Figure 1) in NSCLCs and examines its relationship with the patients' outcome, has not been reported so far. Furthermore, we investigated possible abnormalities of the chromosomal region 9p21–22, which harbors at least three candidate tumor suppressor genes, *CDKN2*, *p15*^{ink4b}, and methylthioadenosine phosphorylase (*MTAP*), and correlated the findings with p16 protein expression.[2,51,52]

The p16-pRb pathway was investigated by IHC, which allows evaluation of the protein expression at a single-cell level.[12,22,40,53] In our approach (see Materials and Methods) a mosaic pattern of staining was not interpreted as abnormal as even in p16- or pRb-positive cell lines a subset of nuclei remained unstained due to cell cycle fluctuations.[54,55] In our study, solely cytoplasmic reactivity of p16 was disregarded. Its significance is unclear to date and has been observed by others.[53,56,57] If cytoplasmic reactivity proves to be specific, one possible explanation is that alteration in subcellular localization can represent a mechanism of p16 inactivation. Wild-type p53 protein has an analogous mechanism of loss of function.[58]

Aberrant p16 was observed in 49% of the carcinomas. This is consistent with certain studies reporting abnormal p16 protein staining in 47% to 51% of NSCLCs,[20,22,25] although other studies reported percentages ranging from 27% to 67%.[13,21,24] This discrepancy may be due to technical parameters of the assays and/or criteria of positivity used by the authors.

To investigate the mechanisms that underlie *CDKN2/p16*^{ink4a} inactivation we examined the chromosomal region 9p21–22 by microsatellite analysis (Figure 2a) and the methylation and structural status of the *CDKN2/p16*^{ink4a} gene by a PCR-based methylation assay and PCR-SSCP, respectively, and then correlated the findings with the results of IHC. A highly significant association was observed between LOH(c) and abnormal p16 protein staining ($P = 0.0001$), suggesting that deletions may represent an important mode of *CDKN2/p16*^{ink4a} gene inactivation. Several groups have investigated *CDKN2/p16*^{ink4a} gene deletions with controversial results.[13,15–17,21,23,25] These differences may be due to contamination of the homogenates by non-neoplastic cells and aneuploidy of tumor cells. By using a microdissection technique we ameliorated the approach, but we

did not completely solve the problem. Furthermore, we observed that 52% of the NSCLCs with p16 loss by IHC were methylated at the 5′CpG island of the first exon of the *CDKN2/p16*^{ink4a} gene (subgroups A2 and A3, Figure 8). This is in agreement with previous results showing a correlation between p16 staining and exon 1 methylation status in primary NSCLCs and NSCLC cell lines.[25,26] PCR-SSCP analysis of exons 1 and 2 in our study did not reveal any minor structural alterations, providing support to previous evidence that intragenic *CDKN2/p16*^{ink4a} alterations are infrequent events in NSCLCs.[15–20,23,25] Thus, overall, 30 of 33 cases (91%) with abnormal p16 protein staining had LOH(c) and/or abnormal methylation status of the *CDKN2/p16*^{ink4a} gene (Figure 8). Therefore, taking together our data and those so far reported it appears that deletions and transcriptional silencing by methylation might be the predominant mechanisms that inactivate *CDKN2/p16*^{ink4a} gene in NSCLCs. The three cases of subgroup A4 with loss of p16 protein expression do not show obvious genetic and epigenetic alterations (Figure 8). One possible explanation is that these microsatellite markers were not sufficient to detect small deletions in the *CDKN2/p16*^{ink4a} region (case 17). Alternatively, the presence of normal contaminating DNA may contribute to a retention pattern in cases with homozygous deletion (cases 17, 29, and 45). A third possibility that could account for loss of protein expression is the presence of mutations outside the examined region; such is the case of the mutation being in the second intron splice donor site, which results in a smaller p16 protein with a reduced half-life, possibly undetectable by IHC.[59] The retention of p16 protein expression in the cases of subgroup B3 suggests either alterations of other TSGs located in the 9p21–22 region and/or a compensatory mechanism by the remaining *CDKN2/p16*^{ink4a} allele (cases 30 and 59).

Deletion mapping of the 9p21–22 region in NSCLCs has been performed by several groups. The frequency of genetic alterations detected ranged from 48% to 68%. These percentages are higher than those reported for *CDKN2/p16*^{ink4a} gene deletions.[13,15–17,21,23,25] Similarly, in the present study LOH was observed in 51% of the samples, which is consistent with the findings presented by other groups[60–63] and, moreover, higher than the frequency of LOH(c) (38%). These results suggest that another TSG(s) might reside in 9p21–22 besides *CDKN2*, *p15*^{ink4b}, and methylthioadenosine phosphorylase (MTAP), which are placed between *D9S171* and *IFNA* loci. This hypothesis is further supported by our deletion-mapping analysis, which revealed LOH at the loci *D9S126* and *D9S162* in 41% and 32% of the informative cases, respectively. Both loci lie 1 cM and 6 cM far from the aforementioned TSGs, respectively (Figure 2a) and recently have been proposed to lie near the location of putative TSGs.[38,64,65] The *talin* gene, also, has recently been mapped in this region.[66] Talin is a critical molecule for the formation of focal adhesions, and its inactivation disassembles many of these structures.[67] The *talin* gene, therefore, is a candidate for a role in NSCLC carcinogenesis. An interesting finding of our study was that 16% of the carcinomas showed MI. This was found more frequently in SCLCs (27%) than in adenocarcinomas (9%) and co-existed in two cases with LOH (Figure 8). MI provides a marker for replication error phenotype (RER+), a recently defined manifestation of genetic instability observed in a wide range of tumors.[68] Cellular populations with RER+ phenotype exhibit elevated mutational rates, which may lead to oncogene and/or oncosuppressor gene deregulation and therefore contribute to tumor development. The data concerning MI in NSCLCs are conflicting with respect to the frequency and the pattern.[43,69,70] Considering the frequency, our percentage is closer to that of Fong et al,[43] who found MI in 6.5% of the cases examined. In that study MI was associated with extensive, concurrent molecular changes in K-*ras* and *p53*. In our study 55% of the cases with MI had *p53* mutations. In two other reports MI occurred in 2%[69] and 34%[70] of NSCLCs. As far as the pattern is concerned, we observed that in most cases affected, MI was restricted to one marker each time. This is in agreement with some studies[43,69] but differs from another study where MI affected multiple markers concurrently.[70] Therefore, more studies are needed to clarify whether MI in NSCLCs merely reflects extensive genetic damage or plays a more important role similar to that observed in hereditary nonpolyposis colorectal cancer (HNPCC).[71]

The incidence of aberrant pRb expression in our analysis was 40% and is the highest reported so far.[12,20–22,25,27–30] Serrano et al has proposed a negative feedback model, showing that inactivation of pRb during G1 leads to increased p16 expression to limit CDK4 activity.[4] Moreover, several studies in various tumors, including NSCLCs, have demonstrated a reciprocal relationship between pRb and p16.[16,20,21,25,72,73] However, in this cohort we noticed an inverse distribution of p16 and pRb proteins in 26 (39%) cases whereas 24 (36%) of the carcinomas showed coincident aberrant expression of both proteins. Simultaneous abnormal p16 and pRb expression has also been reported by Hangaishi et al in primary lymphoid malignancies.[74] As several lines of evidence suggest that functional pRb is essential for cell-cycle inhibition by p16,[75] inactivation of p16 in a cell without functional pRb is not likely to confer additional growth advantage to the cancerous cell. In carcinomas with double hits one possible explanation is that p16 inactivation is an early event and precedes *Rb* mutation. In the latter case neutralization of pRb could contribute to advantageous tumor growth by canceling all of the inhibitory effects of the other cyclin-dependent kinase inhibitors (CDKIs) via pRb.[76] The report of Kishimoto et al, who detected specific allelic loss in *IFNA* and *D9S171* loci in preneoplastic lesions accompanying NSCLCs, enforces the assumption for an early *CDKN2/p16*^{ink4a} deletion in NSCLC carcinogenesis.[77] In this respect, our findings that p16 inactivation was noticed in almost one-half of the carcinomas and its frequency was higher than loss of pRb, besides the lack of association with tumor stage, suggest an early involvement of *CDKN2/p16*^{ink4a} alterations in NSCLC development. This can be supported by several studies reporting no correlation between loss of p16 and clinical stage in primary NSCLCs.[21] Early implication of p16 has been also suggested in head and neck

squamous carcinomas (HNSC), which share many etiological and morphological features with NSCLCs.[78] In contrast to this hypothesis are the results of Okamoto et al, who detected *CDKN2/p16*^{ink4a} mutations only in metastatic and not primary NSCLCs.[14] Alternatively, p16 may participate in other yet unknown pRb-independent pathways. This can be supported by the findings that p16 inactivation causes activation of cyclins D2 and D3, which may act on other substrates besides pRb.[76]

In this cohort of NSCLCs we found co-expression of p53 and MDM2 proteins in ~48% of the cases, thereby confirming our previous findings.[35,36] A highly significant association was also observed between *p53* mutations and p53 IHC ($P = 0.006$), verifying previous reports that show that p53-positive staining in the carcinomas of the upper and lower respiratory tract is strongly indicative of *p53* mutations.[46] Simultaneous expression of p53 and MDM2 has been increasingly reported in a wide variety of tumors.[33,34] Co-detection of MDM2 and mutant p53 (mt p53) protein might represent a mutant p53 gain of function phenotype. Recently, we provided evidence that certain p53 mutants maintain the ability to transactivate the p53 responsive element (p53RE) of the *MDM2* gene.[37] Similar evidence has been reported also by others.[79] Furthermore, we have observed that in certain cases this effect is limited to the p53RE of growth-promoting genes.[80] Alternatively, in cases with inactive or absent p53, the MDM2 protein might be induced via a p53-independent manner. *MDM2* gene amplification is unlikely to represent this p53-independent mechanism as it is a very rare event in lung carcinomas.[35,36,81] The activation of the *MDM2* p53-independent promoter P1 may account for MDM2 overexpression in these cases.[33,34,37] On the other hand, we observed elevated levels of MDM2 and wild-type (wt) p53 protein in 19% of the carcinomas (Table 1). As MDM2 and wt p53 form a negative feedback loop, this immunophenotype might reflect a complex formation between the two molecules that down-regulates the effects of wt p53.[33] However, we should keep in mind that immunohistochemical co-expression of p53 and MDM2 does not necessary imply this complex formation because the proportion of p53 bound to MDM2 is controlled by complicated post-translational events.[82,83] Moreover, recent reports suggest an MDM2-promoted degradation mechanism of wt and mt p53 and a p14^{ARF}-dependent regulation mechanism of MDM2, making the picture of the p53-MDM2 relationship much more complex.[48,49,84] Finally, one cannot exclude the possibility that MDM2 overexpression may simply reflect the activity of wt p53, accumulated in the hypoxic environment of the proliferating cancerous cells.[33,34,46]

After having evaluated independently the p16-pRb and p53-MDM2 pathways we addressed the issue of possible interrelations among impairments of these four molecules. Interestingly, we found two statistically significant associations. Abnormal expression of pRb was correlated with elevated levels of MDM2 ($P = 0.013$) and p53 ($P = 0.01$), respectively. In the first case, MDM2 overexpression could represent an additional mechanism of pRb inactivation, as MDM2 inhibits pRb regulatory function by interacting physically with it.[32] It is unlikely that aberrant pRb staining represents a masking effect due to MDM2-pRb complex formation because the anti-pRb antibody we used and MDM2 recognize different epitopes of pRb.[32] The significance of the association between p53 overexpression and abnormal pRb staining is unclear. Shiio et al showed that wt p53 suppresses *RB1* transcription (Figure 1) and proposed that reduction of pRb would relieve the load of CDKs, thus creating another pathway to down-regulate the activity of pRb and promoting cells to enter S phase.[31] In a similar manner, inactivation of p53 in a cancerous cell might possibly facilitate loss of the *RB1* gene or, *vice versa*, abrogation of pRb, which has a known anti-apoptotic effect, might lead to alteration of the *p53* gene to bypass induction of apoptosis by wt p53.[85] This can be supported by findings in various malignant tumors.[86–88] Furthermore, Kinoshita and co-workers showed that deregulation of the p16/pRb pathway might synergistically increase proliferation activity with altered p53 protein.[21] However, more studies are required to address this point. One of the most important findings of the present study is that multiple disruption (three and four molecules affected) of the p16/pRb/p53/MDM2 network occurred in a large (43%) proportion of NSCLCs. Also, the absence of correlation with clinical stage of the carcinomas suggests that multiple hits of this network may be a relatively early event in the development of a subset of NSCLCs.

The relationship of the alterations detected at the 9p21–22 locus and in each one of the four network proteins, with the patients' clinicopathological parameters and outcomes revealed two probably significant correlations: between smoking, p53 staining ($P = 0.05$), and MAs ($P = 0.04$), respectively. There has been no previous report, to the best of our knowledge, of a correlation between smoking and alterations at the 9p21–22 chromosomal region, although Kishimoto et al observed a tendency for an increased frequency of LOH on 9p in smokers with NSCLCs.[77] A number of studies on NSCLCs have examined the association of p16, pRb, and p53, independently, with smoking habits, histology, lymph node status, stage, and survival, reporting controversial findings. Indeed p16 and/or pRb abnormalities were not associated with adverse prognostic factors in several studies,[12,20,21,25,28,29] although correlation was found in others.[18,22,24,25,30] As far as p53 is concerned, many studies have investigated the implication of p53 in NSCLC carcinogenesis, and it appears that the prognostic significance of p53 alterations is rather weak (reviewed in Ref. 89). The only certain fact is that p53 is frequently affected in NSCLCs and it represents a major target for tobacco derivatives, a finding confirmed in our study as well.[46] Finally, with regard to MDM2, besides our previous studies, there are no available data by other groups.[35,36] We have found no statistical correlation between the various biologically relevant immunophenotypes, with the clinicopathological features and survival of the patients except for two probably significant relationships, between smoking and the p53(P)/MDM2(P) ($P = 0.04$) and p16(Ab)/pRb(Ab)/p53(P)/MDM2(P) ($P = 0.03$) patterns, respectively. The significance of these statistical relationships is not clear and needs more stud-

ies to be determined. However, in view of the wide spectrum of genetic targets identified in NSCLCs,[90] the overlapping and compensatory pathways linking most of them and the role of smoking as an indisputable major causal factor in lung carcinogenesis, it is tempting to suggest that, in a subset of NSCLCs, simultaneous deregulation of the members of this network may represent one way of initiating the oncogenic procedure whereas in other NSCLC subsets alternative molecules may play this role.

Acknowledgment

We thank Dr. P. Kanavaros for helpful criticism on the manuscript. Also, we thank Professor M. Oren, Dr. E. Haupt, and Dr, D. Mitropoulos for critical advice.

References

1. Linnoila RI, Aisner SC: Pathology of lung cancer: an exercise in classification. Lung Cancer. Edited by Johnson BE, Johnson DH. New York, Wiley-Liss, 1995, pp 73–95
2. Cordon-Cardo C: Mutations of cell cycle regulators. Am J Pathol 1995, 147:545–560
3. Haber DA: Splicing into senescence: the curious case of p16 and p19^{ARF}. Cell 1997, 91:551–558
4. Serrano M, Hannon G, Beach D: A new regulatory motif in cell-cycle control causing specific inhibition of cyclin D/CDK4. Nature 1993, 366:704–707
5. Kamb A, Gruis NA, Weaver-Feldhaus J, Liu Q, Harshman K, Tavtigian SV: A cell cycle regulator potentially involved in genesis of many tumor types. Science 1994, 264:436–440
6. Knudson AG: Antioncogenes and human cancer. Proc Natl Acad Sci USA 1993, 90:10914–10921
7. Nobori T, Miura K, Wu DJ, Lois A, Takabayashi K, Carson DA: Deletions of the cyclin-dependent kinase-4 inhibitor gene in multiple human cancers. Nature 1994, 368:753–756
8. Cairns P, Mao L, Merlo A: Rates of the p16 (MTS1) mutations in primary tumours with 9p loss. Science 1994, 265:415–416
9. Okamoto A, Demetrick DJ, Spillare EA, Hagiwara K, Hussain SP, Bennet WP, Forrester K, Gerwin B, Serrano M, Beach DH, Herris CC: Mutations and altered expression of p16INK4 in human cancer. Proc. Natl. Acad. Sci. USA 1994, 91:11045–11049
10. Spruck CH III, Gonzalez-Zulueta M, Shibata A, Simoneau AR, Lin MF, Gonzales F, Tsai YC, Jones PA: p16 gene in uncultured tumours. Nature 1994, 370:183–184
11. Zhang S-Y, Klien-Szanto AJP, Sauter ER, Shafarenko M, Mitsunaga S, Nobori T, Carson DA, Ridge JA, Goodrow TL: Higher frequency of the alterations in the p16/CDKN2 gene in squamous cell carcinoma cell lines than in primary tumours of the head and neck. Cancer Res 1994, 54:5050–50503
12. Reissmann PT, Koga H, Takahashi R, Figlin RA, Holmes C, Piantadosi S, Cardon-Cardo C, Slamon DJ, The Lung Cancer Study Group: Inactivation of the retinoblastoma susceptibility gene in non-small-cell lung cancer. Oncogene 1993, 8:1913–1919
13. Sharipo GI, Edwards CD, Kobzik L, Godleski J, Richards W, Sugarbaker DJ, Rollins BJ: Reciprocal Rb inactivation and p16^{INK4} expression in primary lung cancers and cell lines. Cancer Res 1995, 55: 505–509
14. Okamoto A, Hussain SP, Hagiwara K, Spillare EA, Rusin MR, Demetrick DJ, Serrano M, Hannon GJ, Shiseki M, Zariwala M, Xiong Y, Beach DH, Yokota J, Harris CC: Mutations in the *p16*^{INK4} and *p15*^{INKB} in primary and metastatic lung cancer. Cancer Res 1995, 55:1448–1451
15. Shimizu T, Sekiya T: Loss of heterozygosity at 9p21 loci and mutations of the *MTS1* and *MTS2* genes in human lung cancers. Int J Cancer 1995, 63:616–620
16. Xiao S, Joseph DL, Vijg J, Fletcher JA: Codeletion of *p15* and *p16* genes in primary non-small cell lung carcinoma. Cancer Res 1995, 55:2968–2971
17. Washimi O, Nagatake M, Osada H, Ueda R, Koshikawa T, Seki T, Takahashi T: In vivo occurrence of p16 (MTS1) and p15 (MTS2) alterations preferentially in non-small cell lung cancers. Cancer Res 1995, 55:514–517
18. Nakagawa K, Conrad NK, Williams JP, Johnson BE, Kelley MJ: Mechanism of inactivation of *CDKN2/P16*^{ink4a} and *MTS2* in non-small cell lung cancer and association with advanced stage. Oncogene 1995, 11:1843–1851
19. Rusin MR, Okamoto A, Chorazy M, Czyzewski K, Harasim J, Spillare EA, Hagiwara K, Hussain P, Xiong Y, Demetrick DJ, Harris CC: Intragenic mutations of the *p16*^{INK4}, *p15*^{INKB} and *p18* genes in primary non-small-cell lung cancers. Int J Cancer 1996, 65:734–739
20. Sakaguchi M, Fujii Y, Hirabayashi H, Yoon H-E, Komoto Y, Oue T, Kusafuka T, Okada A, Matsuda H: Inversely correlated expression of p16 and Rb protein in non-small cell lung cancers: an immunohistochemical study. Int J Cancer 1996, 65:442–445
21. Kinoshita I, Dosaka-Akita H, Mishina T, Akie K, Nishi M, Hiroumi H, Hommura F, Kawakami Y: Altered p16^{INK4} and retinoblastoma protein status in non-small cell lung cancer: potential synergistic effect with altered p53 protein on proliferative activity. Cancer Res 1996, 56: 5557–5562
22. Kratzke RA, Greatens TM, Rubins JB, Maddaus MA, Niewoehner DE, Niehans GA, Geradts J: *Rb* and *p16*^{INK4a} expression in resected non-small cell lung tumors. Cancer Res 1996, 56:3415–3420
23. Marchetti A, Buttitta F, Pellegrini S, Bertacca G, Chella A, Carnicelli V, Tognoni V, Filardo A, Angeletti CA, Bevilacqua G: Alterations of *p16(MTS1)* in node-positive non-small cell lung carcinomas. J Pathol 1997, 181:178–182
24. Taga S, Osaki T, Ohgami A, Imoto H, Yoshimatsu T, Yoshino I, Yano K, Nakanishi R, Ichiyoshi Y, Yasumoto K: Prognostic value of the immunohistochemical detection of *p16*^{INK4} expression in non-small cell lung carcinoma. Cancer 1997, 80:389–395
25. Betticher DC, White GRM, Vonlanthen S, Liu X, Kappeler A, Altermatt HJ, Thatcher N, Heighway J: G1 control gene status is frequently altered in resectable non-small cell lung cancer. Int J Cancer 1997, 74:556–562
26. Merlo A, Herman JG, Mao L, Lee DJ, Gabrielson E, Burger PC, Baylin SB, Sydranski D: 5′ CpG island methylation is associated with transcriptional silencing of the tumor suppressor p16/CDKN2/MTS1 in human cancers. Nature Med 1995, 1:686–692
27. Geradts J, Hu S-X, Lincoln CE, Benedict WF, Xu H-J: Aberrant *Rb* gene expression in routinely processed, archival tumor tissues determined by three different anti-Rb antibodies. Int J Cancer 1994, 58:161–167
28. Higashiyama M, Doi O, Kodama K, Yochouchi H, Tateishi R: Retinoblastoma protein expression in lung cancer: an immunohistochemical analysis. Oncology 1994, 51:544–551
29. Shimizu E, Coxon A, Otterson GA, Steinberg SM, Kratzke RA, Kim YW, Fedorko J, Oie H, Johnson BE, Mulshine JL, Minna JD, Gazdar AF, Kaye FJ: Rb protein status and clinical correlation from 171 cell lines representing lung cancer, extrapulmonary small carcinoma, and mesothelioma. Oncogene 1994, 9:2441–2448
30. Xu H-L, Hu S-X, Cagle PT, Moore GE, Benedict WF: Absence of retinoblastoma protein expression in primary non-small cell lung carcinomas. Cancer Res 1991, 51:2735–2739
31. Shiio Y, Yamamoto T, Yamaguchi N: Negative regulation of Rb expression by the p53 gene product. Proc Natl Acad Sci USA 1992, 89:5206–5210
32. Xiao ZX, Chen J, Levine AJ, Modjtahedi N, Xing J, Sellers WR, Livingston DM: Interaction between the retinoblastoma protein and the oncoprotein MDM2. Nature 1995, 375:694–698
33. Piette J, Neel H, Marechal V. Mdm2: keeping p53 under control. Oncogene 1997, 15:1001–1010
34. Haines DS: The mdm2 proto-oncogene. Leuk Lymphoma 1996, 26: 227–238
35. Gorgoulis V, Rassidakis G, Karameris A, Papastamatiou H, Trigidou R, Veslemes M, Rassidakis A, Kittas C: Immunohistochemical and molecular evaluation of the MDM2 gene product in bronchogenic carcinoma. Mod Pathol 1996, 9:544–554
36. Gorgoulis V, Zoumpourlis V, Rassidakis G, Karameris A, Rassidakis A, Spandidos DA, Kittas C: A molecular and immunohistochemical

study of the MDM2 protein isoforms and *p53* gene product in bronchogenic carcinoma. J Pathol 1996, 180:129–137
37. Gorgoulis VG, Zacharatos PV, Manolis E, Ikonomopoulos JA, Damalas A, Lamprinopoulos C, Rassidakis GZ, Zoumpourlis V, Kotsinas A, Rassidakis AN, Halazonetis TD, Kittas C: Effects of p53 mutants derived from lung carcinomas on the p53 responsive element (p53RE) of the MDM2 gene. Br J Cancer 1998, 77:378–384
38. Wiest JS, Franklin WA, Otstot JT, Forbey K, Varella-Garcia M, Rao K, Drabkin H, Gemmill R, Ahrent S, Sidransky D, Saccomanno G, Fountain JW, Anderson MW: Identification of a novel region of homozygous deletion on chromosome 9p in squamous cell carcinoma of the lung: the location of a putative tumor suppressor gene. Cancer Res 1997, 57:1–7
39. World Health Organization: The World Health Organization histologic typing of lung tumours. Am J Clin Pathol 1982, 77:123–136
40. Geradts J, Wilson PA: High frequency of aberrant p16ink4A expression in human breast cancer. Am J Pathol 1996, 149:15–20
41. Whetsell L, Maw G, Nadon N, Ringer D, Schaefer F: Polymerase chain reaction microanalysis of tumors from stained histological slides. Oncogene 1995, 7:581–585
42. Davis LG, Dibner MD, Battey JF: Basic Methods in Molecular Biology. Amsterdam, Elsevier Science Publishing, 1986
43. Fong KM, Zimmermann PV, Smith PJ: Microsatellite instability and other molecular abnormalities in non-small cell lung cancer. Cancer Res 1995, 55:28–30
44. Chaubert P, Guillou L, Kurt A-M, Bertholet M-M, Metthez G, Leisinger H-J, Bosman F, Shaw F: Frequent *p16*^{INK4} (*MTS1*) gene inactivation in testicular germ cell tumors. Am J Pathol 1997, 151:859–865
45. Gorgoulis V, Zoumpourlis V, Rassidakis G, Karameris A, Barbatis C, Spandidos DA, Kittas C: Molecular analysis of p53 gene in laryngeal pre-malignant and malignant lesions: p53 protein immunohistochemical expression is positively related to proliferating cell nuclear antigen labelling index. Virchows Arch 1995, 426:339–344
46. Greenblatt MS, Bennett WP, Hollstein M, Harris CC: Mutations in the *p53* tumour suppressor gene: clues to cancer etiology and molecular pathogenesis. Cancer Res 1995, 54:4855–4878
47. Merlo A, Mabry M, Gabrielson E, Vollmer R, Baylin SB, Sidransky D: Frequent microsatellite instability in primary small cell lung cancer. Cancer Res 1993, 54:2098–2101
48. Pomerantz J, Shreiber-Agus N, Liegeois N, Silverman A, Alland L, Chin L, Potes J, Chen K, Orlow I, Lee H-W, Cordon-Cardo C, DePindo RA: The ink4a tumor supppressor gene product, p19^{ARF}, interacts with MDM2 and neutralizes MDM2's inhibition of p53. Cell 1998, 92:713–723
49. Zhang Y, Xiong Y, Yarbrourgh WG: ARF promotes MDM2 degradation and stabilizes p53: *ARF-INK4a* locus deletion impairs both the Rb and p53 tumor suppression pathways. Cell 1998, 92:725–734
50. Otterson GA, Kleif SN, Chen W, Coxon AB, Kaye FJ: CDKN2 gene silencing in lung cancer by DNA hypermethylation, and kinetics of p16INK4 protein induction by 5-aza 2′ deoxycytidine. Oncogene 1995, 11:1211–1216
51. Haber DA: Splicing into senescence: the curious case of p16 and p19^{ARF}. Cell 1997, 91:555–558
52. Olopade OI, Pomykala HM, Hagos F, Sveen LW, Espinosa R III, Dreyling MH, Gursky S, Stadler WM, Le Beau MM, Bolander SK: Construction of a 2.8-megabase yeast artificial chromosome contig and cloning of the human methylthioadenosine phosphorylase gene from the tumor suppressor region on 9p21. Proc Natl Acad Sci USA 1995, 92:6489–6493
53. Geradts J, Kratzke RA, Niehans GA, Lincoln CE: Immunohistochemical detection of the cyclin dependent kinase inhibitor 2/multiple suppressor gene 1 (CDKN2/MTS1) product p16ink4A in archival human solid tumors: correlation with retinoblastoma protein expression. Cancer Res 1995, 55:6006–6011
54. Tam SW, Stay JW, Pagano M: Differential expression and cell cycle regulation of the cyclin-dependent kinase 4 inhibitor p16^{INK4}. Cancer Res 1994, 54:5816–5820
55. Xu H-J, Hu S-X, Benedict WF: Lack of nuclear RB protein staining in G0/middle G1 cells: correlation to changes in total RB protein level. Oncogene 1991, 6:1139–1146
56. Lukas J, Parry D, Aagaard L, Mann DJ, Bartkova J, Strauss M, Peters G, Bartek J: Retinoblastoma protein dependent cell-cycle inhibition by the tumour suppressor p16. Nature 1995, 375:503–506
57. Okamoto A, Detnetrick DJ, Spillare EA, Hagiwara K, Hussain SP, Bennet WP, Forrester K, Gerwin B, Serrano M, Beach DH, Harris CC: Mutations and altered expression of p16INK4 in human cancer. Proc Natl Acad Sci Usa 1994, 91:11045–11049
58. Zambetti GP, Levine AJ: A comparison of the biological activities of wild type and mutant p53. FASEB J 1993, 7:855–865
59. Shapiro GI, Park JE, Edwards CD, Mao L, Merlo A, Sidransky D, Ewen ME, Rollins BJ: Multiple mechanisms of p16^{INK4A} inactivation in non-small cell lung lines. Cancer Res 1995, 55:6200–6209
60. Merlo A, Gabrielson E, Mabry M, Vollmer R, Baylin SB, Sydranski D: Homozygous deletion on chromosome 9p and loss of heterozygosity on 9p, 6p, and 6q in primary human small cell lung cancer. Cancer Res 1994, 54:2322–2326
61. Packenham JP, Taylor JA, White CM, Anna CH, Barrett JC, Devereux TR: Homozygous deletions at chromosome 9p21 and mutation analysis of *p16* and *p15* in microdissected primary non-small cell lung cancers. Clin Cancer Res 1995, 1:687–690
62. Shimizu T, Sekiya T: Loss of heterozygosity at 9p21 loci and mutations of the *MTS1* and *MTS2* genes in human lung cancers. Int J Cancer 1995, 63:616–620
63. Mead LJ, Gillespie MT, Hung JY, Rane US, Rayeroux KC, Irving LB, Campbell LJ: Frequent loss of heterozygosity in early non-small cell lung cancers at chromosome 9p21 proximal to the *CDKN2a* gene. Int J Cancer 1997, 71:213–217
64. Vos S, Miller C, Takeuchi S, Combart A, Cho S, Koeffler H: Alteration of CDKN2 (p16) in non-small cell lung cancer. Genes Chromosomes & Cancer 1995, 14:164–170
65. Neville EM, Stewart M, Myskow M, Donnelly RJ, Field JK: Loss of heterozygosity at 9p23 defines a novel locus in non-small cell cancer. Oncogene 1995, 11:581–585
66. Gilmore AP, Ohanian V, Spurr NK, Critchley DR: Localisation of the human gene encoding the cytoskeletal protein talin to chromosome 9p. Hum Genet 1995, 96:221–224
67. Albiges-Rizo C, Frachet P, Block MR: Down regulation of talin alters cell adhesion and the processing of the $\alpha 5\beta 1$ integrin. J Cell Sci 1995, 108:3317–3329
68. Jiricny J: Colon cancer and DNA repair: have mismatches met their match? Trends Genet 1994, 10:164–168
69. Peltomaki P, Lothe RA, Aaltonen LA, Pylkkanen L, Nystrom-Lathi M, Secura R, David L, Holm R, Ryberg D, Haugen A, Brogger A, Borresen A-L, de la Chapelle A: Microsatellite instability is associated with tumors that characterize the hereditary non-polyposis colorectal carcinoma syndrome. Cancer Res 1993, 53:5853–5855
70. Shridhar V, Siegfried J, Hunt J, del Mar Alonso M, Smith DI: Genetic instability of microsatellite sequences in many non-small cell lung carcinomas. Cancer Res 1994, 54:2084–2087
71. Kinzler KW, Vogelstein B: Lessons from hereditary colorectal cancer. Cell 1996, 87:159–170
72. Yeager T, Stadler W, Belair C, Puthenveettil J, Olopade O, Reznikoff C: Increased p16 levels correlate with pRb alterations in human urothelial cells. Cancer Res 1995, 55:493–497
73. Otterson GA, Kratzke RA, Coxon A, Kim YW, Kaye FJ: Absence of p16^{INK4} protein is restricted to the subset of lung cancer lines that retains wild type RB. Oncogene 1994, 9:3375–3378
74. Hangaishi A, Ogawa S, Imamura N, Miyawaki S, Miura Y, Uike N, Shimazaki C, Emi N, Takeyama K, Hirosawa S, Kamada N, Kobayashi Y, Takemoto Y, Kitani T, Toyama K, Ohtake S, Yazaki Y, Ueda R, Hirai H: Inactivation of multiple tumor-suppressor genes involved in negative regulation of the cell cycle, MTS1/p16^{INK4A}, MTS2/p15^{INK4B}, p53, and Rb genes in primary lymphoid malignancies. Blood 1996, 87: 4949–4958
75. Medema RH, Herrera RE, Lam F, Weinberg RA: Growth suppression by p16^{ink4} requires functional retinoblastoma protein. Proc Natl Acad Sci USA 1995, 92:6289–6293
76. Bernards R: E2F: a nodal point in cell cycle regulation. Biochem Biophys Acta 1997, 1333:M33–M40
77. Kishimoto Y, Sugio K, Hung JY, Virmani AK, McIntire DD, Minna JD, Gazdar AF: Allele-specific loss in chromosome 9p loci in preneoplastic lesions accompanying non-small-cell lung cancers. J Natl Cancer Inst 1995, 87:1224–1229
78. El-Naggar AK, Lai S, Clayman G, Lee J-KJ, Luna MA, Goepfert H, Batsakis JG: Methylation, a major mechanism of p16/CDKN2 gene inactivation in head and neck squamous carcinoma. Am J Pathol 1997, 151:1767–1774
79. Lianes P, Orlow I, Zhang Z-F, Oliva MR, Sarkis AS, Reuter VE, Cor-

don-Cardo C: Altered patterns of MDM-2 expression in human bladder cancer. J Natl Cancer Inst 1994, 86:1325–1330
80. Zacharatos P, Gorgoulis V, Kotsinas A, Kanavaros P, Zoumpourlis V, Veslemes M, Halazonetis T, Kittas C: Modulation of wild-type p53 activity by mutant p53 R273H depends on the p53 responsive element (p53RE): a comparative study between the p53REs of the *MDM2*, *WAF1/Cip1* and *Bax* genes in lung cancer environment. Abstract presented at the 9th p53 Workshop, Crete, May 9 to 14, 1998
81. Marchetti A, Buttitta F, Pellegrini S, Merlo G, Chella A, Angeletti CA, Bevilacqua G: mdm2 gene amplification and overexpression in non-small cell lung carcinoma with accumulation of the p53 protein in the absence of p53 gene mutation. Diagn Mol Pathol 1995, 4:93–97
82. Momand J, Zambetti GP: Analysis of the proportion of p53 bound to mdm-2 in cells with defined growth characteristics. Oncogene 1996, 12:2279–2289
83. Shieh S-Y, Ikeda M, Taya Y, Prives C: DNA damage-induced phosphorylation of p53 alleviates inhibition by MDM2. Cell 1997, 91:325–334
84. Haupt Y, Maya R, Kazaz A, Oren M: Mdm2 promotes the rapid degradation of p53. Nature 1997, 387:296–299
85. White E: p53, guardian of Rb. Nature 1994, 371:21–22
86. Murakami Y, Hirayashi K, Hirohashi S, Sekiya T: Aberrations of the tumor suppressor p53 and the retinoblastoma genes in human hepatocellular carcinomas. Cancer Res 1991, 51:5520–5525
87. Cheng J, Hass M: Frequent mutations in the p53 tumor suppressor gene in human leukemia T-cell lines. Mol Cell Biol 1990, 10:5502–5509
88. Williams BO, Remington L, Albert DM, Mukai S, Bronson RT, Jacks T: Cooperative tumorigenic effects of germline mutations in Rb and p53. Nature Genet 1994, 7:480–484
89. Kalemkerian GP: Biology of lung cancer. Curr Opin Oncol 1994, 6:147–155
90. Groeger AM, Esposito V, Mueller MR, Caputi M, Kaiser HE, Giordano A: Advances in the understanding of lung cancer. Anticancer Res 1997, 17:2519–2522